



UNIVERSITY OF LEEDS

This is a repository copy of *Comparison of cohesive powder flowability measured by Schulze Shear Cell, Raining Bed Method, Sevilla Powder Tester and new Ball Indentation Method*.

White Rose Research Online URL for this paper:
<http://eprints.whiterose.ac.uk/93316/>

Version: Accepted Version

Article:

Zafar, U, Hare, C, Calvert, G et al. (5 more authors) (2015) Comparison of cohesive powder flowability measured by Schulze Shear Cell, Raining Bed Method, Sevilla Powder Tester and new Ball Indentation Method. *Powder Technology*, 286. pp. 807-816. ISSN 0032-5910

<https://doi.org/10.1016/j.powtec.2015.09.010>

© 2015, Elsevier. Licensed under the Creative Commons Attribution-NonCommercial-NoDerivatives 4.0 International
<http://creativecommons.org/licenses/by-nc-nd/4.0/>

Reuse

Unless indicated otherwise, fulltext items are protected by copyright with all rights reserved. The copyright exception in section 29 of the Copyright, Designs and Patents Act 1988 allows the making of a single copy solely for the purpose of non-commercial research or private study within the limits of fair dealing. The publisher or other rights-holder may allow further reproduction and re-use of this version - refer to the White Rose Research Online record for this item. Where records identify the publisher as the copyright holder, users can verify any specific terms of use on the publisher's website.

Takedown

If you consider content in White Rose Research Online to be in breach of UK law, please notify us by emailing eprints@whiterose.ac.uk including the URL of the record and the reason for the withdrawal request.



eprints@whiterose.ac.uk
<https://eprints.whiterose.ac.uk/>

**Comparison of Cohesive Powder Flowability Measured by Schulze Shear Cell, Raining
Bed Method, Sevilla Powder Tester
and New Ball Indentation Method**

U. Zafar¹, G. Calvert¹, C. Hare¹, M. Ghadiri^{1*},
R. Girimonte², B. Formisani²,
M.A.S. Quintanilla³, J.M. Valverde³,

¹ The Institute of Particle Science & Engineering, University of Leeds, Leeds, LS2 9JT, UK

² Dipartimento di Ingegneria Chimica e dei Materiali, Università della Calabria, 87030
Arcavacata di Rende (Cosenza), Italy

³ Dept. of Electronics and Electromagnetism Faculty of Physics. University of Seville. Avda.
Reina Mercedes s/n 41012 Seville. Spain

* Corresponding author

Prof. Mojtaba Ghadiri

Tel: +44 (0) 113 343 2406

Fax: +44 (0)113 343 2405

Email address: M.Ghadiri@leeds.ac.uk

Abstract

Poor powder flow leads to many problems during manufacturing and can lead to inaccurate dosing and off-specification products. Powder flowability is commonly assessed under

relatively high applied loads using shear cells by characterising the unconfined yield strength at a range of applied loads. For applied stresses below 1 kPa, it becomes increasingly difficult to obtain reliable values of the unconfined yield strength. The bulk cohesion and tensile strength of the powder is then obtained by extrapolating the yield locus to zero and negative loads. However, the reliability of this approximation for a given material is not known. To overcome this limitation, techniques such as the Raining Bed Method, Sevilla Powder Tester and the newly-developed Ball Indentation Method may be used.

In this paper, we report our measurement results of the tensile strength of glass beads, α -lactose monohydrate and various sizes of fluid catalytic cracking powders determined by the Sevilla Powder Tester and Raining Bed Method and compare them with those inferred from the Schulze Shear Cell. The results of the latter are also compared with those of the Ball Indentation Method. The outcome suggests that in the case of shear cell tests, the extrapolation of the yield locus to lower or negative loads is unsafe. The ball indentation enables the characterisation of highly cohesive powders at very low compressive loads; however extrapolation to negative loads is still not reliable. In contrast, the Sevilla Powder Tester and Raining Bed Methods are able to characterise the tensile strength directly, but high bulk cohesion poses difficulties as the internal bed failure needs to be analysed in order to reliably estimate the tensile strength. These methods provide a better understanding of powder flow behaviour at low stresses, thus enabling a greater control of manufacturing processes.

Keywords: Powder flowability, Powder characterisation, Ball indentation,

1. Introduction

An important factor when performing bulk powder flowability measurements is whether the instrument can replicate the stresses that are applicable to the system of interest. With commercial testers, it is often a challenge to investigate systems with stresses much less than 1 kPa. This is highly desirable in a number of applications, such as filling small bags, tableting shoes and capsules and Dry Powder Inhalers (DPIs). There are many techniques [1] which are used in different industries for the characterisation of powder flowability. The shear cell is the most commonly used method and is used in this study for bench marking. It gives an indirect measurement of bulk cohesion and tensile strength. The knowledge of these mechanical properties of a powder is important in understanding storage and handling issues of cohesive powders, e.g. in arching and dispersion. The tensile strength of a powder is determined from the yield locus [2] by extrapolating it to the tensile region, as it is otherwise impossible to apply tensile stresses experimentally in a shear cell. This is often done by fitting a straight line to the yield locus. However, the yield locus tends to curve downwards for cohesive powders at low stresses, so in these conditions such a procedure yields an overestimated value of the tensile strength [3]. In that case, the yield locus of a powder can be better approximated by Warren-Spring equation [4].

The most commonly used shear cells suitable for analysing the flowability of bulk solids are the Jenike powder tester [5], Peschl shear cell [6] and Schulze ring shear tester [2]. However, the measurement of flowability at low stresses is difficult, although Schulze and Wittmair [7]

report measurements at stresses of around 50 Pa. Also when dealing with cohesive powders, where even small variations in inter-particle contact forces have a large effect, these testers do not reproduce the initial state of filling reliably and reproducibly [8].

There are test methods developed which can directly measure the tensile yield stress. The split cell tester is a commercial apparatus which consists of a ring shaped cell with a plunger for compaction of sample powders [1]. In this technique a horizontal tensile stress is applied to pull the sample apart and the tensile strength is measured at a given applied stress. Based on a similar principle, the lifting lid tester measures the tensile strength of the sample by pulling it vertically in the opposite direction to compaction [9]. These two techniques are unable to achieve a uniform stress distribution inside the sample, hence they have a poor reproducibility for fine cohesive powders [10].

Two recently developed test methods, which can directly measure the tensile yield stress are the Sevilla Powder Tester (SPT) [10] and the Raining Bed Method (RBM) [11]. In these devices the bed failure is induced by manipulating the pressure drop across the bed. Advantages of SPT and RBM are that the initial state of the bed is reproducible and the tensile strength can be determined at low levels of stress.

In another recent development, ball indentation on a bed of cohesive powders has been applied for assessing the flowability of a small quantity of powders at very low stress levels. Although this method cannot measure the tensile strength directly, it provides a simple and quick method to assess the resistance of the powder bed to plastic deformation, hence giving

a measure of flowability. This paper examines the performance of these three new test methods and compares them against that of the well-established shear cell method.

2. Experimental Procedures

Sevilla Powder Tester (SPT) This is an automated powder characterisation apparatus which requires a relatively small amount of powder, and is shown in Figure 1. It includes a porous base (a sintered metal gas distributor of 5 μm pore size), supporting a powder sample within a vertical cylinder dimension of 44.5 mm diameter and 170 mm height made of polycarbonate material. A pre-weighed sample is poured into the vessel to a level which gives an aspect ratio (H/D) about equal or smaller than unity in order to minimise the wall effect. A dry air flow is pumped into the powder bed from the base whilst the pressure drop across the bed is measured by a differential pressure transducer. The flow rate is increased so that the powder bed is fluidised, bringing the sample to a reproducible stress state. During this process an electromagnetic shaker attached to the bottom of the apparatus is operated to break the formation of channels within the powder bed [12]. The gas flow is then stopped and reversed to compress the powder bed. The pressure across the bed is increased to give a pre-specified applied stress at the base of the bed σ_1 ;

$$\sigma_1 = W / A + \Delta P_0 \quad (\text{Eq.1})$$

where W is the weight of the sample, A is the cross-sectional area of the bed and ΔP_0 is the pressure drop across the bed. The gas flow direction is again reversed to the upward direction

and slowly increased; the pressure drop at which a fracture at the bed base is detected is used to calculate the tensile failure stress. An important advantage of the SPT is that the initial state of the bed is reproducible. The measurement of the tensile failure stress can be made under small applied loads.

The Raining Bed Method This is the other test method for measuring the tensile strength of the powder bed. The method was first proposed by Buysman and Peersman [13] and further applied by Seville and Clift [14] and Formisani et al. [11]. This method has a few similarities to the SPT. The rain-off experiments of this paper were performed in a transparent column of Perspex with an internal diameter of 54 mm and 400 mm high. As sketched in Figure 2, each end of this column is connected to a plenum chamber bearing a high pressure drop porous plate, so that air can be admitted to the column through either of these distributors by acting on a three-way valve, as required by the procedure adopted for the bed support experiment. The column is provided with four pressure taps each connected to a transducer to allow pressure drop measurements: PT1 and PT4 are placed symmetrically, level with the two gas distributors. PT2 and PT3 are located 66 mm apart within the bed height, with PT2 being 46 mm from PT1. The bed mass was 350 g for glass ballotini, giving a de-fluidised bed height of 150 mm, and an aspect ratio H/D larger than 2.2. In order to switch from fluidisation to rain-off experiments, the column can be rotated upside down around a horizontal axis. Measurements of the differential pressure drop were carried out both across the whole height of the bed (ΔP_{1-4}) and the internal section between PT2 and PT3 (ΔP_{2-3}).

Initially the powder is fluidised to remove any stress history (shown in Figure 3a) and to measure the minimum fluidisation velocity. After the air flow is switched off, the bed is then

tapped to reduce the bed voidage to a desired fraction. A downward flow of air is then introduced and the flow rate is increased to a level, which maintains a stable bed condition whilst the bed is rotated 180° without causing any change in the bed packing. After rotation the air flow rate is upward supporting the bed in upside-down position. The air flow rate is then gradually reduced until it reaches a critical velocity, U_{ro} at which the bed fails and a plug falls down. The position/plane of failure is video recorded. A force balance on the plug would yield the tensile strength of the failed plane. The initial pressure drop across the whole bed (ΔP_{1-4}) for the raining bed tests is in the range of 4.0-12.0 kPa for glass ballotini, 0.6-3.4 kPa for Respitose and 6.6-9.4 kPa for the FCC samples. At U_{ro} , if the powder has no cohesion, the bed will fail layer wise from its surface. However, if cohesion is present, the tensile strength resists raining, even when the pressure drop is less than the bed weight. Referring to Figure 3, at the bed failure point, the upward fluid drag, F_{drag} and tensile force, F_c , balance the weight of the plug that falls down, W_{plug} , i.e.

$$A[\Delta P_{plug(Uro)} - \sigma_T] = W_{plug} \quad (\text{Eq. 2})$$

where, σ_T is the macroscopic tensile strength acting on the horizontal failure plane of cross-sectional area of the bed, A , $\Delta P_{plug(Uro)}$ is the pressure drop of powder bed across the plug height H_{plug} at the rain-off point. W_{plug} can be measured by collecting the plug and weighing it, or alternatively as used here it can be determined from the pressure drop across bed height H_{2-3} at minimum fluidisation condition, U_{mf} , i.e. $W_{plug} = A\Delta P_{plug(Umf)}$.

$$\Delta P_{plug(Umf)} - \Delta P_{plug(Uro)} = \sigma_T \quad (\text{Eq. 3})$$

Now considering that the pressure drop per unit height is constant, Eq.3 can be expressed in terms of ΔP_{2-3} , (which is actually measured), as given by Eq.4.

$$\sigma_T = [\Delta P_{\text{plug}(U_{mf})} - \Delta P_{\text{plug}(U_{ro})}] H_{\text{plug}} / H_{2-3} \quad (\text{Eq. 4})$$

U_{mf} is the minimum fluidisation velocity, U_{ro} is the rain-off velocity and H_{plug} is the height of the failed plug, whose value is obtained from the analysis of the images recorded by a video camera (Sony HDR-HC7E) during the experiment. Although not perfectly even, the newly formed bed surface after the fall of the plug is smooth, planar and horizontal, so that evaluation of the mass of H_{plug} proves relatively easy. The SPT and RBM are based on similar principles, the only difference being that the plug weight acts in opposite directions in the two cases at the failure point. However, the determination of the equivalent applied stress in RBM is not straight forward as the stress state may vary due to the rotation of cylinder.

Ball Indentation Method A new method, capable of handling measurements at low stresses less than 1 kPa and requiring a relatively small amount of powder, has been introduced by Hassanpour and Ghadiri [15]. This method is based on indentation hardness measurements carried out on compacted bulk powder beds. It gives a measure of resistance to plastic deformation and is well-developed for hardness measurement of continuum solids. However, extension to testing of cohesive powder beds has only recently been analysed [16], [17] and [18]. In this method a spherical ball indenter penetrates into a bed of powder and with the increase in load F , the indentation depth h is continuously recorded to produce a depth/load curve as shown in Figure 4. During the unloading stage, only the elastic deformation of the sample recovers and when the load reaches zero the final value of the indentation depth has a final value h_f larger than zero. The depth h_c , representing the elastically-recovered depth, can

be calculated by estimating the tangent to the initial elastic part of the unloading curve. The slope of the tangential line gives the stiffness, which determines the location of h_c on the penetration depth axis. The hardness of the powder bed can then be calculated by the expression:

$$H = \frac{F_{\max}}{A} \quad (\text{Eq. 3})$$

where F_{\max} is the maximum indentation load and A is the projected area of the impression of the indenter which can be obtained using;

$$A = \pi(d_b h_c - h_c^2) \quad (\text{Eq. 4})$$

where d_b is the diameter of the indenter and h_c is the intercept of the tangent to the unloading curve.

Ball indentation was investigated using the Instron 5566 mechanical testing machine. The samples were first pre-consolidated in a die by a stainless steel piston using a 10 N load cell which has a resolution of 0.25 mN. The cylindrical die used in this testing is made of polytetrafluoroethylene (PTFE) in order to minimise wall friction and has an inner diameter of 20 mm. The strain rate is kept constant at 10^{-3} s^{-1} , therefore testing at quasi-static conditions. The pre-consolidated samples were then subjected to indentation using a high precision spherical ball indenter of 2.8 mm supplied by Sigmund Lindner GmbH. In the indentation hardness testing, the volume of material under yielding condition is surrounded by an elastically deformed region and cannot easily flow, causing some constraining of powder flow. Therefore, hardness is usually larger than the plastic yield stress. In continuum solids, a linear relationship is commonly assumed: $H = CY$ where H is the indentation hardness, Y is the yield stress and C is termed as the constraint factor. For powders, C

depends on single particle properties such as particle shape, roughness and friction coefficient [15].

For the determination of the bulk mechanical failure properties of the powders using the standard shear cell testing procedure, the Schulze ring shear tester (RST-XS, Dr.-Ing. Dietmar Schulze, Wolfenbittel) has been used and the detailed procedure has been described by Schulze [2]. A family of yield loci is plotted as a function of the consolidation major principal/applied stress, and a linear extrapolation to the abscissa is made to determine the tensile strength.

Despite their literature presence and great potential for evaluation of powder cohesion, these new techniques are not been commercially available and have not been evaluated and compared against the standard and common method of shear cell testing. In this paper, a first attempt is made to compare the outcomes of these methods for a number of powder materials.

2.1 Materials

The materials used in this study are spherical glass ballotini (a free-flowing model material), three different size distributions of Fluid Catalytic Cracking (FCC) equilibrium catalyst (commonly used in the petroleum industry) and Respitose[®] SV003 (a sieved grade α -lactose monohydrate used in the pharmaceutical industry as excipient). The characteristics of the particle size distributions of the powders are given in Table 1 and were determined by laser diffraction using the Mastersizer 2000 (Malvern Instruments, UK) in a wet dispersion environment.

3. Results

3.1 Shear cell

There are a number of methods to predict the tensile strength of the powder. The most commonly used one is the linear approximation, but this might be inadequate to describe the behaviour of fine cohesive powders at low values of τ and σ [20]. The materials used in this comparative study exhibit free flowing behaviour based on the ratio of unconfined yield strength and major principal stress defined by flow function (ffc), shown in Table (2), determined using Schulze (RST-XS) ring shear tester. Related data are given in the Appendix. The relationship between the shear and normal stresses for Respitose SV003 sample is shown in Figure 5 for an applied stress of 6 kPa. It can be seen that in the case of the Respitose SV003 sample, the shear stress has a linear relationship with normal stress for a given pre-shear stress condition. A similar trend was observed for all the other materials tested at different applied stresses, as shown in Appendix. Therefore, the yield locus can be approximated by a linear function given by Coulomb's law [21]. Using linear extrapolation, the tensile strength of the test materials was determined and is shown in Figure 6 as a function of the applied stress, where a clear trend is observed. Each test was repeated three times and the error bars show the maximum and minimum values. Glass ballotini and Respitose exhibit a higher tensile strength as compared to more free flowing FCC materials. The tensile strengths for a given major principal stress are very similar for the different sizes of FCC, though there is a slight increase as particle size is reduced. For Respitose the slope of the yield locus becomes marginally shallower as the pre-shear stress is increased.

3.2 Sevilla Powder Tester (SPT)

An example of the raw data obtained in SPT for the gas pressure drop across the bed to cause failure as a function of the superficial gas velocity is shown in Figure 7 for the 45-63 μm FCC sample. The critical gas velocity at which the powder bed fractures is marked by a sharp fall in the pressure drop. It was observed for all the materials that the fracture of the bed started near the base of the powder bed. The tensile strength measured for different applied stress levels for all the materials is shown in Figure 8. Comparing the data of Figures 6 and 8 for the shear cell and SPT, the trend of tensile strength for these materials is very similar. The magnitude of the tensile strength of Respitose (0.28- 0.40 kPa) and glass beads (0.13- 0.35 kPa) measured by the shear cell is greater than that of the SPT (Figure 8). However, for FCC powders both of these tests provide similar magnitude of the tensile strength. Another difference is that the SPT provides a greater differentiation than the shear cell between the tensile strength of the different size distributions of FCC. The variation of tensile strength with major principal stress is approximately linear for all materials in the shear cell (Figure 6). This is also the case with the SPT at higher applied stresses (Figure 8). However at lower stresses the tensile strength drops slightly below linearity in the SPT.

A notable feature of the SPT is its ability to measure the failure stress at low applied stress, typically much less than 1 kPa. Fine powders, such as glass beads and Respitose used here, exhibit a higher tensile strength due to the higher ratio of the attractive van der Waals force to particle weight as compared to the more free flowing FCC powders. Also, it is expected that as the sieve cut size decreases, the tensile strength increases.

3.3 Raining Bed Method

The results in the case of Respirose sample obtained from this method are shown in Figures 9 (a) and (b). The pressure drop across the whole bed (ΔP_{1-4}) from the top of the gas distributor plate to the free board above the bed surface and pressure drop (ΔP_{2-3}) across a length of the powder bed (H_{2-3}) give nearly the same U_{mf} . Referring to Figure 9 (b), as the velocity is reduced from the high end with the bed in a raining position (i.e. up-side down), the pressure drop first reaches a value corresponding to U_{mf} , but the inter-particle adhesion prevents the bed failing until the superficial velocity is reduced to U_{ro} . At this point the tensile strength is calculated according to Eq.4.

The tensile strengths obtained for all the materials tested as calculated from Eq.(4) are shown in Figure 10 as a function of applied stress on the powder bed. Different levels of packing fraction are achieved by tapping the bed gently, and the corresponding pressured drop which gives the same party fraction is used for calculation of applied stress. These diagrams show that, as seen before, the tensile strength increases with the increase in applied stress. Amongst all the materials tested, glass beads exhibit the greatest tensile strength. In the case of the FCC samples, only FCC 45-63 has a measureable tensile strength as shown in Figure 10. This is the finest cut of this material (45-63 μm) whereas the other two samples (63-75 and 75-90 μm) behave as cohesionless materials with no measurable tensile strength by this method.

3.4 Ball Indentation Method

In this method, the samples are consolidated to certain normal stress and the indentation tests are carried out. The hardness measurements as a function of applied stress for glass beads and Respitose samples are shown in Figure 11. The error bars in Figure 11 indicate the span between maximum and minimum value based on three experiments.

It can be seen from Figure 11 that BIM can give reliable measurements at low applied stresses. In both cases of Respitose SV003 and glass beads, the hardness increases with applied stress. The trend observed in indentation experiments is similar to that in SPT and RBM experiments with glass beads material showing higher tensile strength and hardness due to greater bulk cohesion, followed by Respitose SV003.

4. Discussion

In Figures 12-14, the tensile strength as a function of applied stress is given for all the materials measured by the SPT, RBM and the extrapolated tensile strength, inferred from the Schulze ring shear tester. The data obtained with the different techniques cover a wide range of stress conditions. In all the tests it is seen that, as expected, the tensile strength increases with applied stress. It is also observed that the tensile strength values are reasonably coherent, as they line up along a unique trend. However, an exact agreement is not seen and this is indicative of the difficulty of measuring bulk powder behaviour by different techniques, due to its marked sensitivity on the initialisation conditions and stress history.

The use of different initialisation procedures in these techniques influences the measurement, since it is well known that bulk powder failure is influenced by stress history, which can only be brought to a reproducible state if the powder is effectively taken to a fluidised regime, as in the case of SPT and raining bed technique [20] or sheared until steady state flow is achieved in the shear cell [21]. On the other hand, the tensile strength given by the shear tester is not a direct measure, but an extrapolation of data taken from a shear test.

The tensile strength comparison between the shear cell and RBM as a function of measured applied stress is shown in Figures 12 and 14. A good qualitative agreement is seen between the shear cell, SPT and RBM, i.e. the rate of increase in tensile strength is similar for all tests. However, the trend for RBM is mixed. In almost all cases it measures a lower value of the tensile strength. This highlights the difficulty of comparing measurements made between different techniques, wherein the powder has been subjected to different conditions. As shown in Figures 12-14 for the glass beads, Respitose SV003 and FCC, respectively, the tensile strength given by SPT and RBM has been characterised at stress states less than those possible with the shear cell.

Notwithstanding a certain scatter, the agreement between shear cell, SPT and RBM data for Respitose and FCC powder is good for these tests in the common range of the applied stresses. Furthermore, the tensile strength variation with applied stress follows a similar gradient. In the case of glass beads powders, shown in Figure 12, notable differences are observed for the RBM data. A good agreement with the trend obtained by the other techniques is observed as far as the material is endowed with some tensile strength, so that the fall of a plug of solids is observed. That occurs only with the 45-63 μm cut of FCC,

whereas for the other two size cuts particles rain down individually, according to the behaviour typical of cohesionless materials. Therefore, for FCC 63-75 and 75-90 μm Eq. 4 simply does not apply and no result can be reported in Figure 14. It should be noted that the tensile strength is measured by these techniques at different points within the bed. In the SPT fracture occurs generally near the bottom of the bed where the applied stress reaches its maximum value, the bed is more compacted [22, 23]. On the other hand, fracture in the RBM occurs at planes closer to the free surface, where there is less wall effect and porosity could be different from that of the bed failure location in the SPT. In contrast, the yield plane in the shear tester is unknown and failure might occur at different planes in different runs. Generally, and since the distribution of stresses in granular materials is highly heterogeneous, an important information that should be known in any test is the location of the failure/fracture plane, which should ideally occur in a reproducible way. The main issue in comparing the three techniques is differences in the stress history. Figures 12-14 show that nevertheless they give a consistent representation of the variation of the tensile strength, considering the wide range of stress state conditions tested.

In Figures 15 and 16, comparisons are made between the resistance to deformation represented by hardness results, obtained by BIM, as a function of applied stress and the unconfined yield strength, obtained from shear cell tests for glass beads and Respitose SV003, respectively. A correlation exists for both materials between the hardness and unconfined yield strength down to a certain low stress level of approximately 3 kPa, as the shear cell could not provide measurements for these free-flowing materials at very low stresses. It is also noted that both the indentation hardness and unconfined yield strength increase linearly with the applied stress. The correlation between the two test results may be

expressed by the constraint factor (C), i.e. the ratio of measured hardness to the yield stress. The hardness of the powder bed can be linked to the tensile strength of the material indirectly through the unconfined yield strength and internal friction angle determined by the shear cell. A more rigorous comparison amongst the techniques requires a detailed analysis of the mechanics of the bulk failure. This may be best addressed by the Distinct Element Method (DEM), which is however outside the scope of the present work.

5. Conclusions

The tensile strength of a range of powders has been measured directly by the SPT and the RBM and indirectly by the Schulze ring shear tester and BIM. The SPT, RBM and BIM have the ability to measure bulk properties at very low stresses. This is most useful to applications such as mechanical dry powder inhalers and dry powder dispersion for sizing. Qualitatively the test methods provide similar results for the tested powders, with the rankings of powders in terms of tensile strength being the same for each technique. The tensile strength increases with applied stress for all powders in all techniques. The tensile strength measured by the shear cell is also greater than that measured by the SPT and RBM. For FCC this increases as particle size is reduced, with the sensitivity to particle size being least for the shear cell. For glass beads and Respitose the bed hardness measured by BIM correlates well with the unconfined yield strength measured in the shear cell. The differences in the values of the tensile strength as measured by different techniques show that the stress history of the powder and method of measurement are influential. It is thus of paramount importance to analyse in detail the conditions of powder flow for each application in order to choose the most

appropriate test, in which the powder is subjected to conditions closer to those expected in practice. Further work should utilise DEM to provide a more in-depth understanding of the reasons for the differences between the measurements using these techniques.

6. References

- [1] J. Schwedes, Review on testers for measuring flow properties of bulk solids. *Granular Matter* 5, (2003); 1-45.
- [2] D. Schulze, Discussion of Testers and Test Procedures. *Powders and Bulk Solids*, Springer Berlin Heidelberg. 2008:163–198.
- [3] A. Vasilenko, S. Koynov, B.J. Glasser, F.J. Muzzio, Role of consolidation state in the measurement of bulk density and cohesion. *Powder Technology*. 2013, 71(7), 2791.
- [4] M. D. Ashton, R. Farley and F. H. H. Valentin. An Improved Apparatus for Measuring the Tensile Strength of Powders. *Journal of Scientific Instruments* (1964), 41 (12): 763-765.
- [4] A. Jenike, Storage and flow of solids. Salt Lake City; 1964:Bull. No. 123.
- [5] M. D. Ashton, R. Farley and F. H. H. Valentin. An Improved Apparatus for Measuring the Tensile Strength of Powders. *Journal of Scientific Instruments* (1964), 41 (12): 763-765.
- [6] I. A. S. Z. Peschl, Quality control of powders for industrial application. Proceedings of 14th annual Powder & Bulk Solids Conference, Chicago. 1989:517–536.

- [7] D. Schulze, A. Wittmaier, Flow properties of highly dispersed powders at low consolidation stresses, *Chem. Eng. Technol.* 26 (2003) pp. 133-137.
- [8] A. Verlinden, Experimental assessment of shear testers for measuring flow properties of bulk solids, PhD-Thesis, Univ. of Bradford, UK (2000).
- [9] H. Kamiya, A. Kimura, T. Yokoyama, M. Naito, G. Jimbo, Development of a split-type tensile-strength tester and analysis of mechanism of increase of adhesion behaviour of inorganic fine powder bed at high-temperature conditions. *Powder Technology*, (2002); 239-245.
- [10] J.M. Valverde, A. Castellanos, A. Ramos, A.T. Pérez, M.A. Morgan, P. Watson, An automated apparatus for measuring the tensile strength and compressibility of fine cohesive powders. *Review of Scientific Instruments*. 2000;71(7):2791.
- [11] B. Formisani, P. Bernardo, R. Girimonte, A. Minnicelli, The bed support experiment in the analysis of the fluidization properties of fine solids. In: *Proceedings of the conference 4th World Congress on Particle Technology*. Sydney (Australia); 2002:373.
- [12] A. Castellanos, The relationship between attractive interparticle forces and bulk behaviour in dry and uncharged fine powders. *Advances in Physics*. 2005; 54:263–376.
- [13] P.J. Buysman, G. Peersman, *Proc. Int. Symp On Fluidization*. Netherlands Univ. Press. 1967:38.
- [14] J.P.K. Seville, R. Clift, The effect of thin liquid layers on fluidisation characteristics. *Powder Technology*. 1984; 37(1):117-129.

- [15] A. Hassanpour, M. Ghadiri, Characterisation of Flowability of Loosely Compacted Cohesive Powders by Indentation. *Particle & Particle Systems Characterization*. 2007;24(2):117–123.
- [16] M. Pasha, C. Hare, A. Hassanpour, M. Ghadiri, Analysis of ball indentation on cohesive powder beds using distinct element modelling. *Powder Technology*. 2013;233:80–90.
- [17] U. Zafar, Assessing Flowability of Cohesive Powders by Ball Indentation. Ph.D thesis, University of Leeds. 2013.
- [18] M. Pasha, Modelling of Flowability Measurement of Cohesive Powders Using Small Quantities. Ph.D thesis, University of Leeds. 2013.
- [19] A. Castellanos, J.M. Valverde, M.A.S. Quintanilla, The Sevilla Powder Tester : A Tool for Characterizing the Physical Properties of Fine Cohesive Powders at Very Small Consolidations. *KONA*, 2004;22(22):66–81.
- [20] J. M. Valverde, A. Castellanos, M. A. S. Quintanilla, The memory of granular materials., *Contemporary Physics*, 2003; 44 (5): 389-399.
- [21] R.M. Neddermann, *Statics and Kinematics of Granular Materials*. London, Cambridge University Press. 1992.
- [22] M. A. S. Quintanilla, A. Castellanos, J. M. Valverde, Correlation between bulk stresses and interparticle contact forces in fine powders. *Physical Review*, 2001; 64 (31301): 1-9.

- [23] M.A.S. Quintanilla, J.M. Valverde, A. Castellanos, Adhesion force between fine particles with controlled surface properties., *AIChE J*, 2006; 52 (5): 1715-1728.

7. Appendix:

Table A1: List of pre-shear and normal stresses used for all the test materials in shear cell experiments.

Pre-Shear Stress (kPa)	Normal Stress (kPa)
2	1.8
	1.6
	1.4
	1.2
	1.0
3	2.6
	2.2
	1.8
	1.4
	1.0
4	3.5
	3.0
	2.5
	2.0
	1.5
	1.0
5	4.4
	3.8
	3.2
	2.6
	2.0

	1.0
6	5.2
	4.4
	3.6
	2.8
	2.0
	1.0

Table A2: Results of shear cell for Respirose sample at different pre-shear stresses.

Pre-shear Stress (kPa)	Major Principal Stress (kPa)	Unconfined Yield Strength (Pa)	Cohesion (Pa)	Estimated Tensile Strength (Pa)
2.0	4.2	419.3	136.5	287.8
3.0	6.1	423.3	144.2	303
4.0	7.9	407.0	160.3	338.5
5.0	10.0	460.0	175.2	365.8
6.0	12.1	467.0	190.9	401.1

Table A3: Results of shear cell for Glassbeads sample at different pre-shear stresses.

Pre-Shear Stress (kPa)	Major Principal Stress (kPa)	Unconfined Yield Strength (Pa)	Cohesion (Pa)	Estimated Tensile Strength (Pa)
2.0	3.3	691.0	158.3	213.5
3.0	4.8	666.0	180.8	245.7
4.0	6.3	719.0	201.7	278.3
5.0	7.9	780.0	222.3	305.1
6.0	9.4	915.0	258.3	348.3

Table A4: Results of shear cell for FCC-56 sample at different pre-shear stresses.

Pre-Shear Stress (kPa)	Major Principal Stress (kPa)	Unconfined Yield Strength (Pa)	Cohesion (Pa)	Estimated Tensile Strength (Pa)
2.0	3.2	99.7	37.5	77.2
3.0	4.7	123.7	41.0	94.9
4.0	6.2	119.7	52.1	109.7
5.0	7.8	141.3	59.2	123.6
6.0	9.3	133.7	65.1	139.3

Table A5: Results of shear cell for FCC-70 sample at different pre-shear stresses.

Pre-Shear Stress (kPa)	Major Principal Stress (kPa)	Unconfined Yield Strength (Pa)	Cohesion (Pa)	Estimated Tensile Strength (Pa)
2.0	3.3	72.0	40.4	83.1
3.0	4.7	103.3	38.0	77.1
4.0	6.3	130.7	45.6	93.9
5.0	7.8	133.3	52.9	108.7
6.0	9.3	141.3	59.0	122.0

Table A6: Results of shear cell for FCC-87 sample at different pre-shear stresses.

Pre-Shear Stress (kPa)	Major Principal Stress (kPa)	Unconfined Yield Strength (Pa)	Cohesion (Pa)	Estimated Tensile Strength (Pa)
2.0	3.2	95.0	24.3	48.8
3.0	4.7	79.0	34.0	69.6
4.0	6.3	85.3	38.2	77.4
5.0	7.8	114.7	50.7	105.8
6.0	9.2	119.7	55.3	115.9

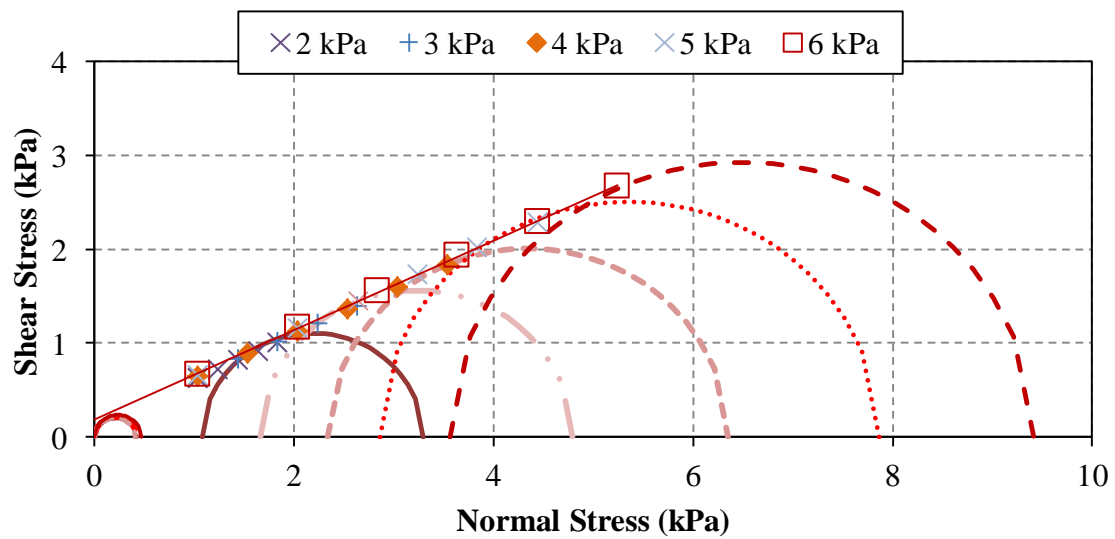


Figure A1: Relationship between shear stress and normal stress for glass beads sample for a number of pre-shear stresses, measured by Schulze RST-XS ring shear tester.

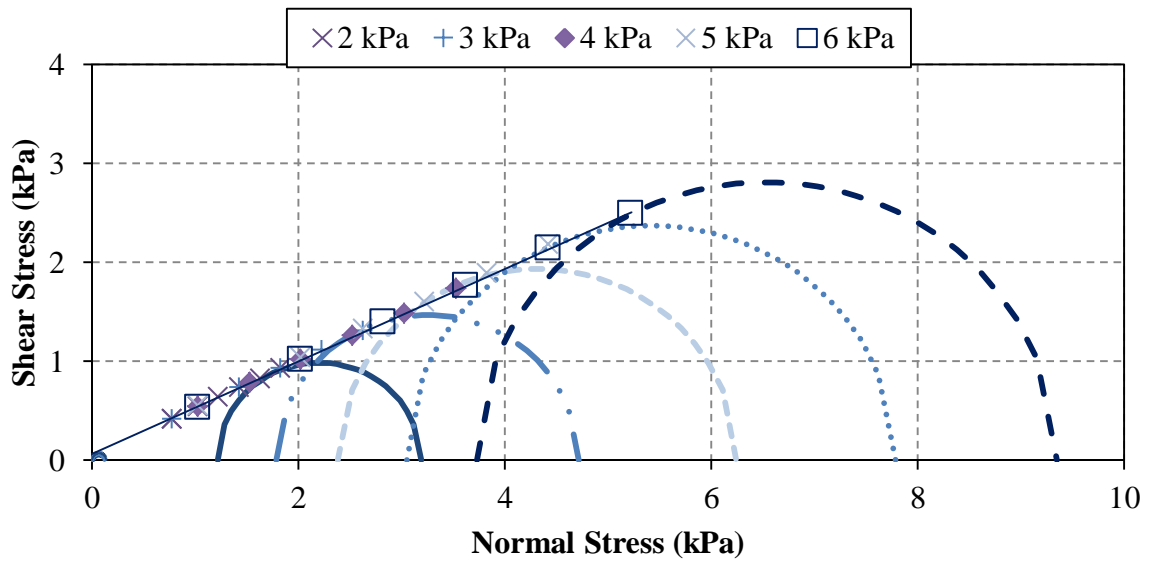


Figure A2: Relationship between shear stress and normal stress for FCC 45-63 μm sample for a number of pre-shear stresses, measured by Schulze RST-XS ring shear tester.

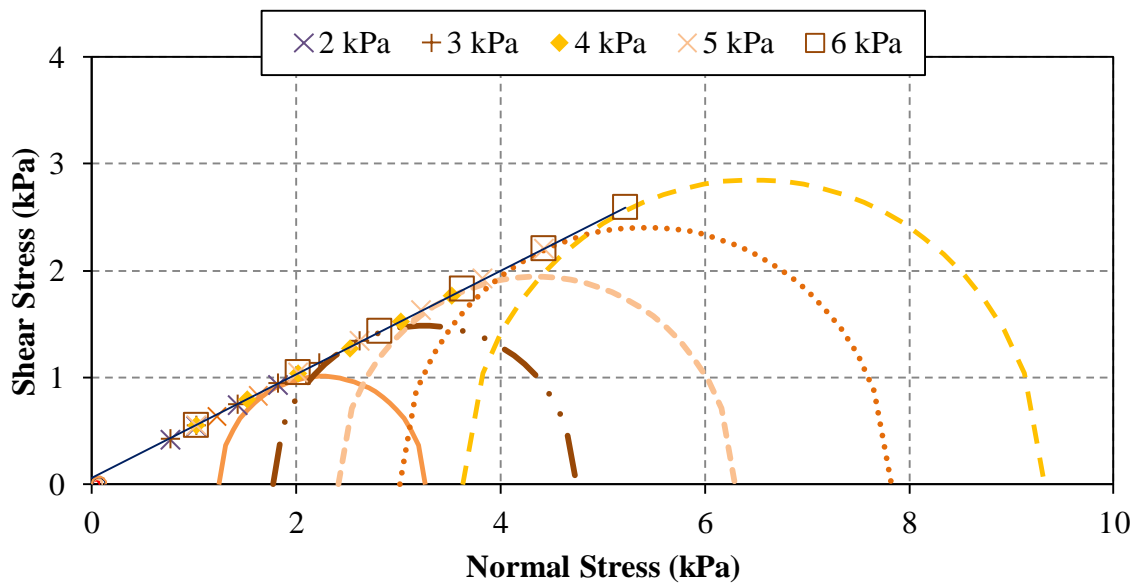


Figure A3: Relationship between shear stress and normal stress for FCC 63-75 μm sample for a number of pre-shear stresses, measured by Schulze RST-XS ring shear tester.

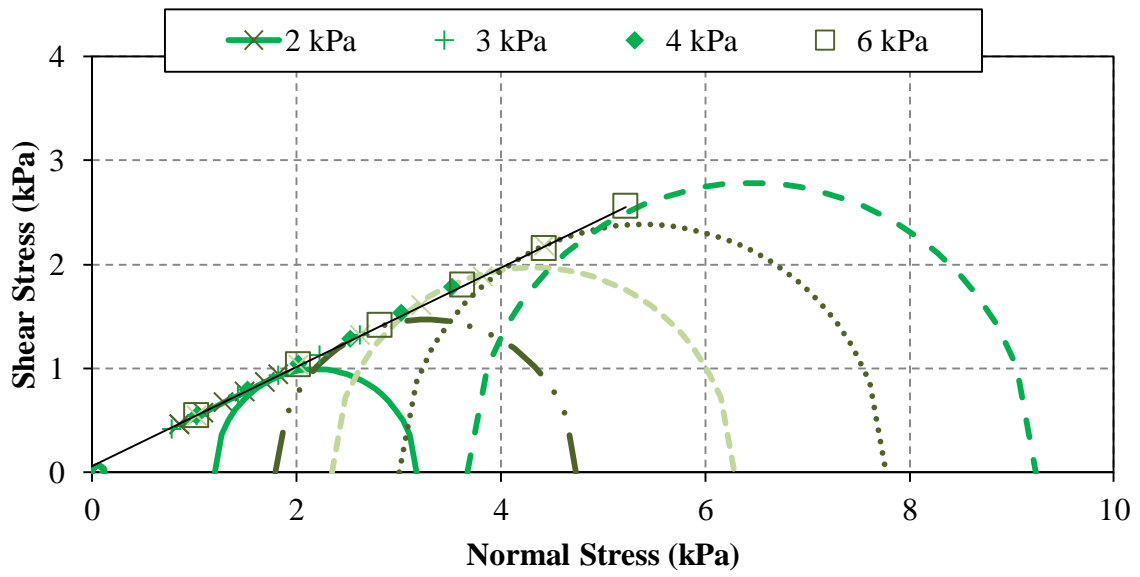


Figure A4: Relationship between shear stress and normal stress for FCC 75-90 μm sample for a number of pre-shear stresses, measured by Schulze RST-XS ring shear tester.

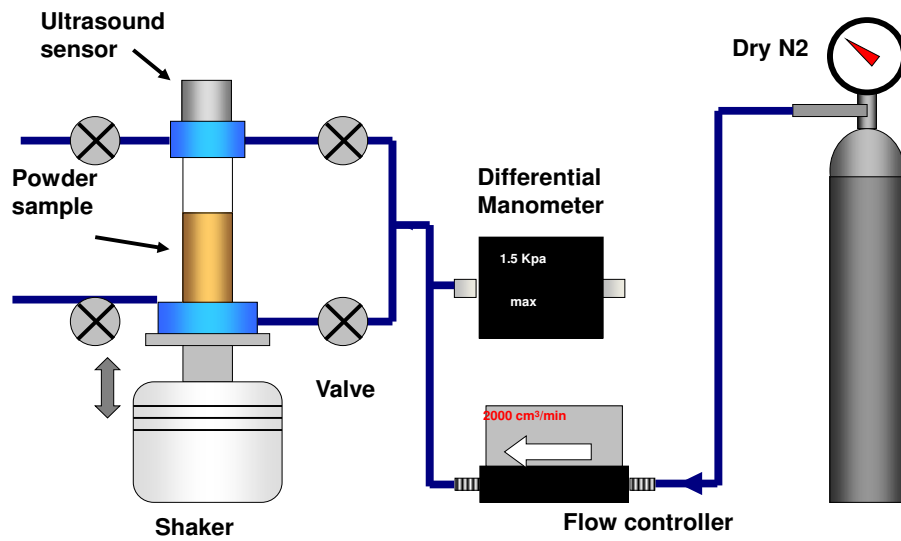


Figure 1: Sevilla Powder Tester setup. [9]

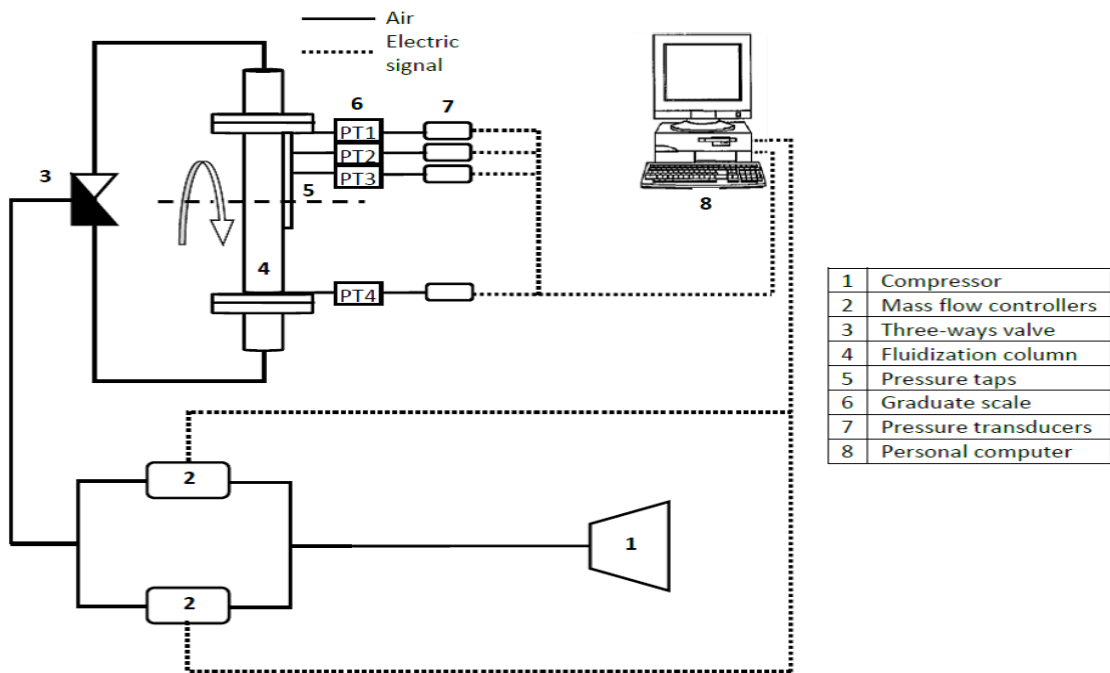


Figure 2: Raining Bed Method experimental setup [11].

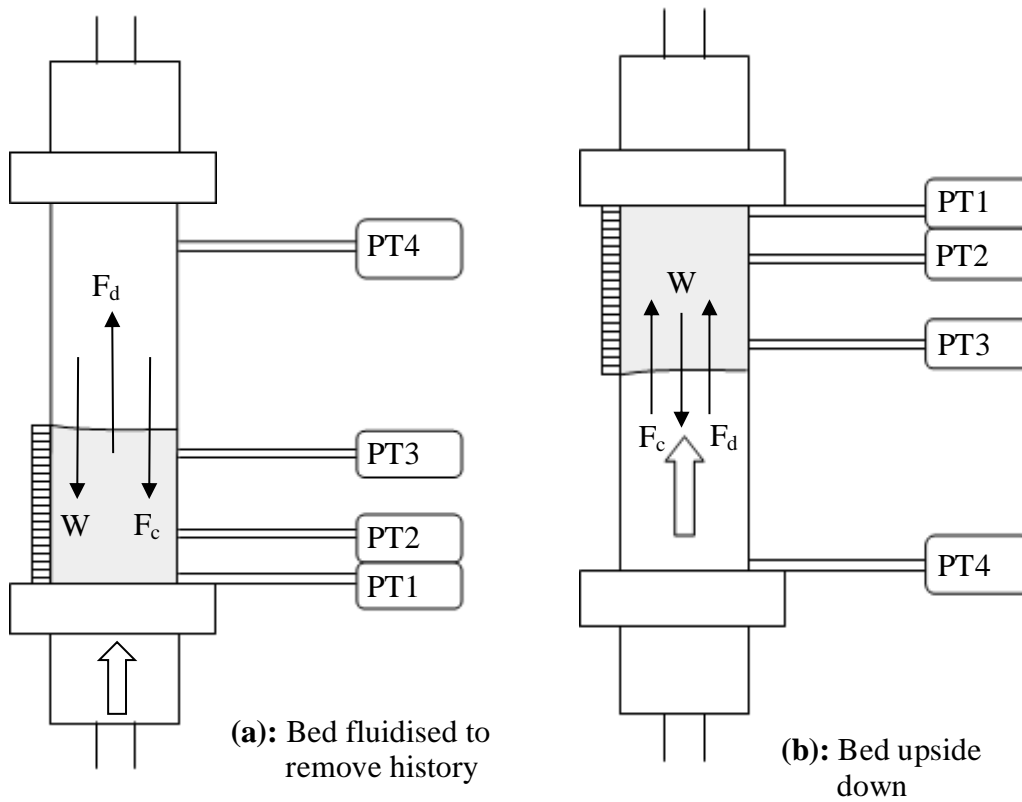


Figure 3: Flow condition for fluidisation and rain-off.

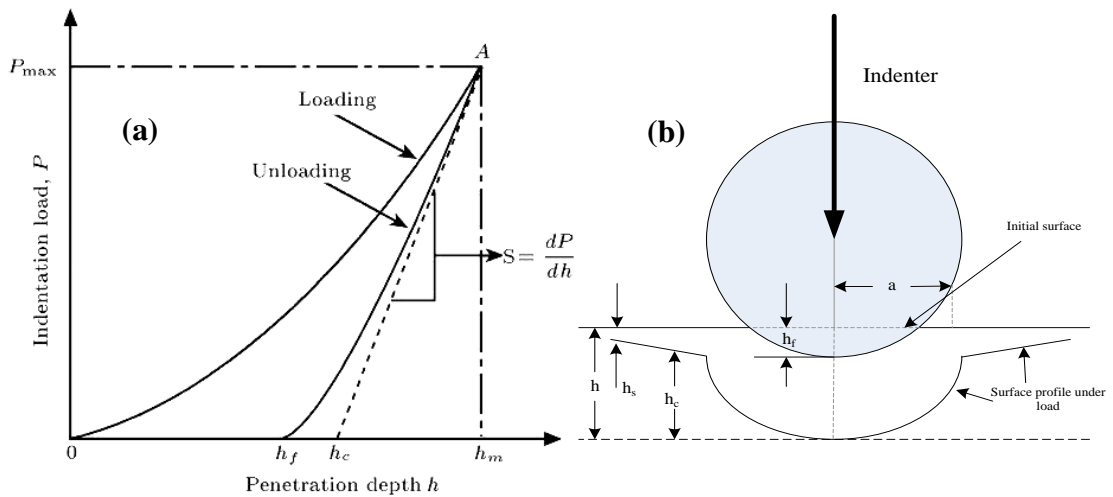


Figure 4: (a) Loading/Unloading curve (b) Indentation on powder bed.

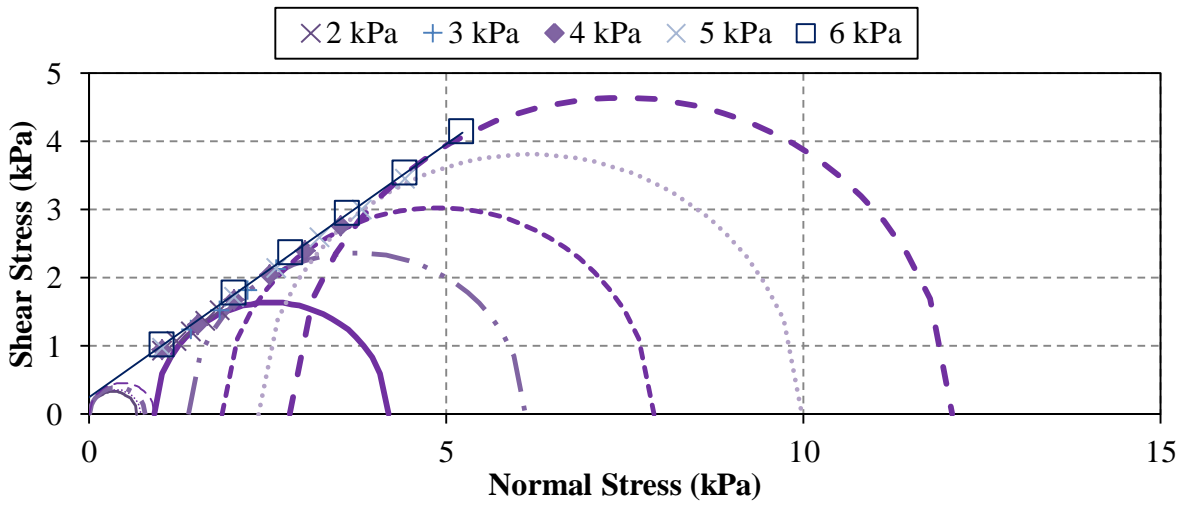


Figure 5: Relationship between shear stress and normal stress for Respitose SV003 sample for a number of pre-shear stresses, measured by Schulze RST-XS ring shear tester.

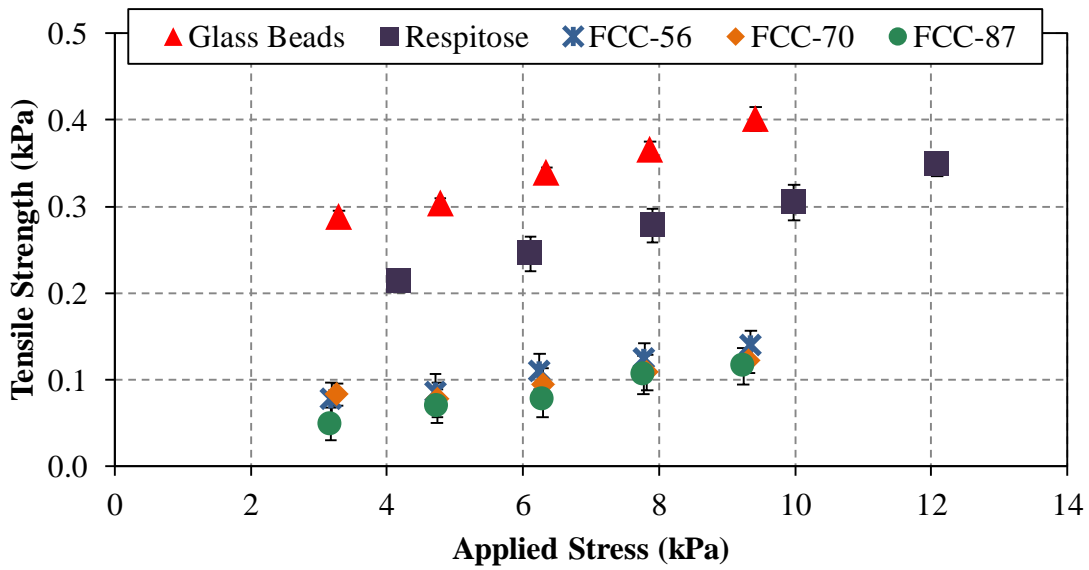


Figure 6: Relationship between inferred tensile strength and applied stress for all the test materials obtained with Schulze RST-XS ring shear tester.

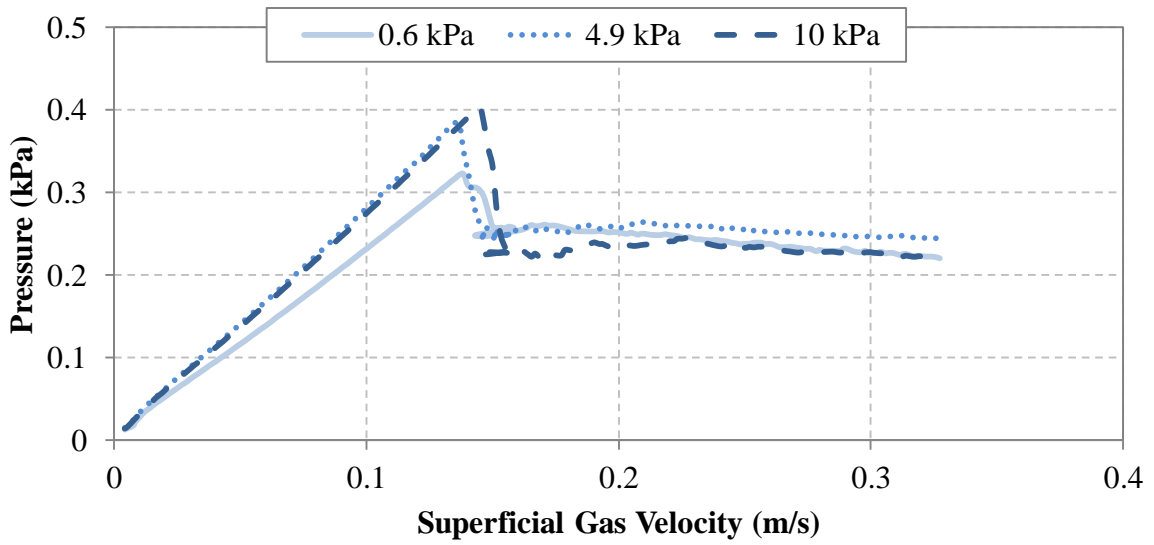


Figure 7: Gas pressure drop versus superficial gas velocity to cause bed failure for a given powder mass and at different applied stresses for 45-63 μm FCC sample.

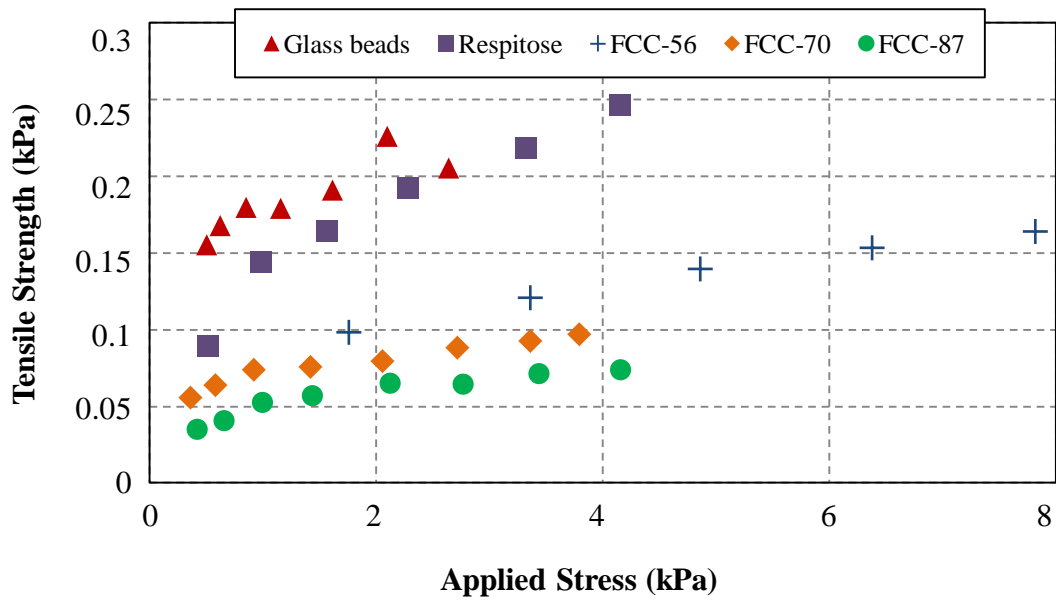


Figure 8: Tensile strength as a function of applied stress for materials tested in SPT.

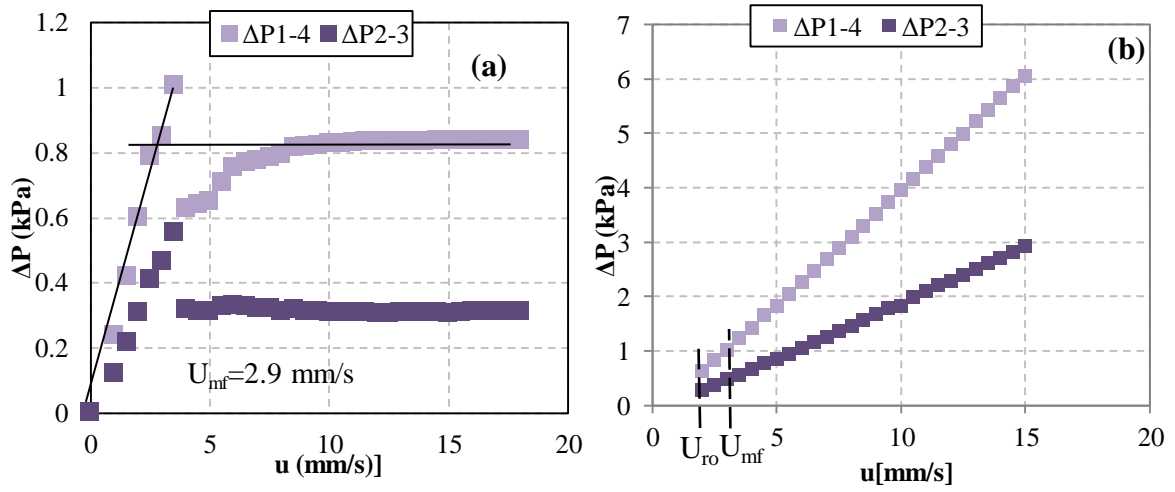


Figure 9: Pressure drop as a function of superficial gas velocity for Respirose (a) fluidisation; (b) raining bed

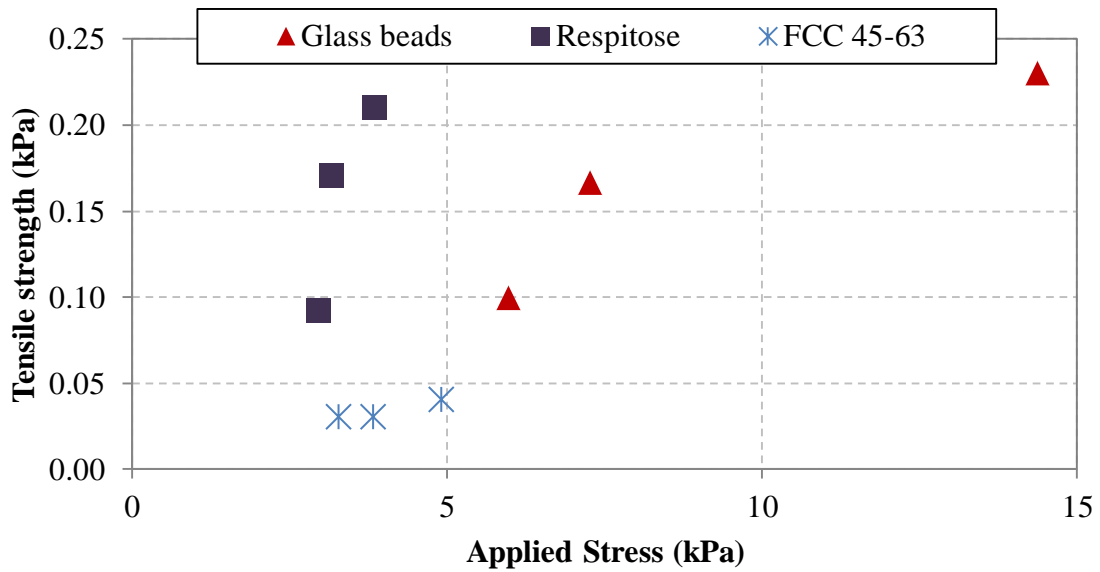


Figure 10: Tensile strength as a function of applied stress for the test materials obtained from RBM.

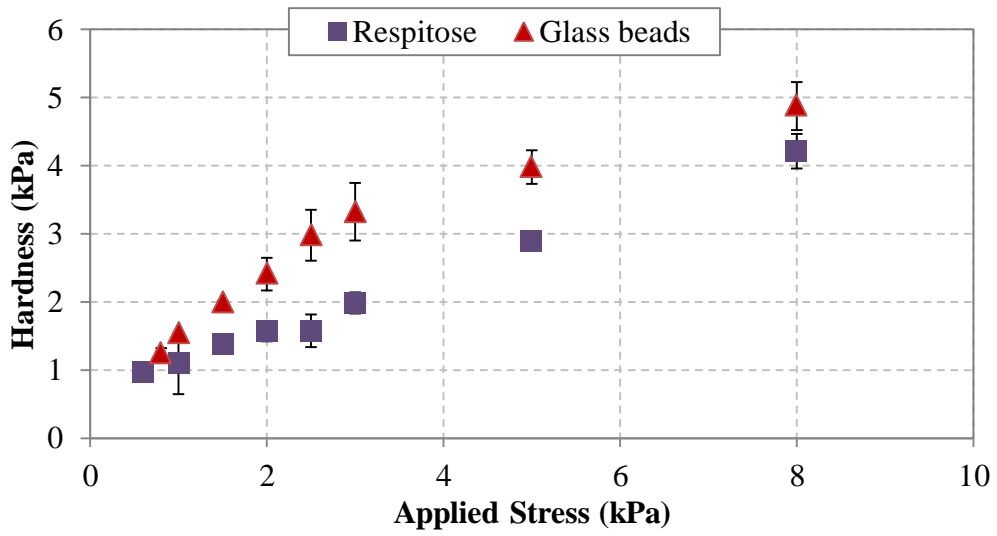


Figure 11: Hardness as a function of applied stress for Respitose SV003 and glass beads from BIM.

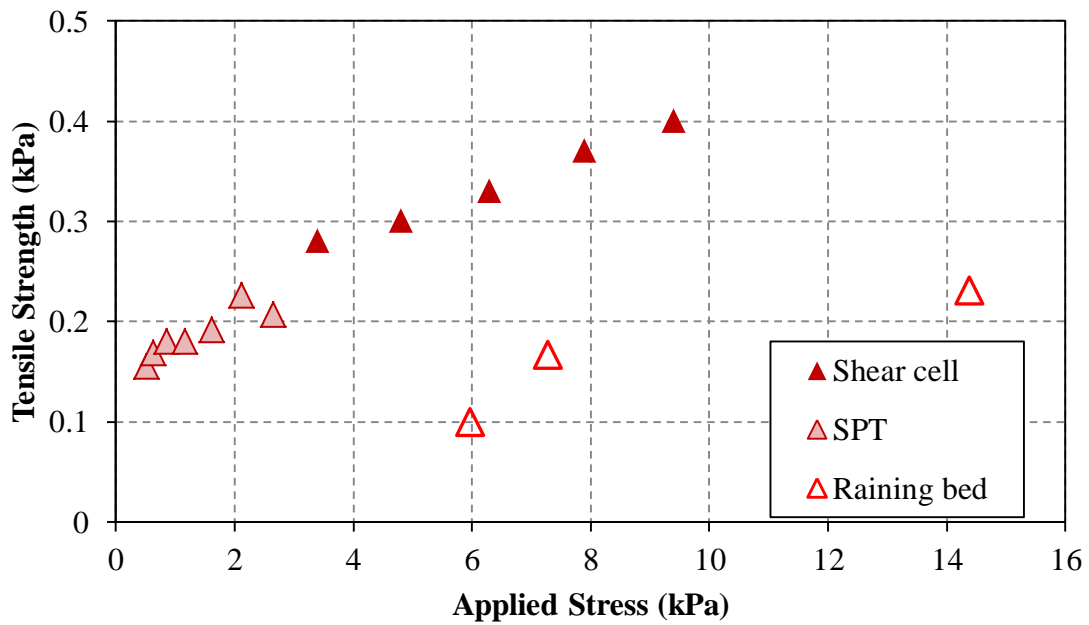


Figure 12: Comparison between shear cell, Raining bed and SPT techniques for glass beads sample.

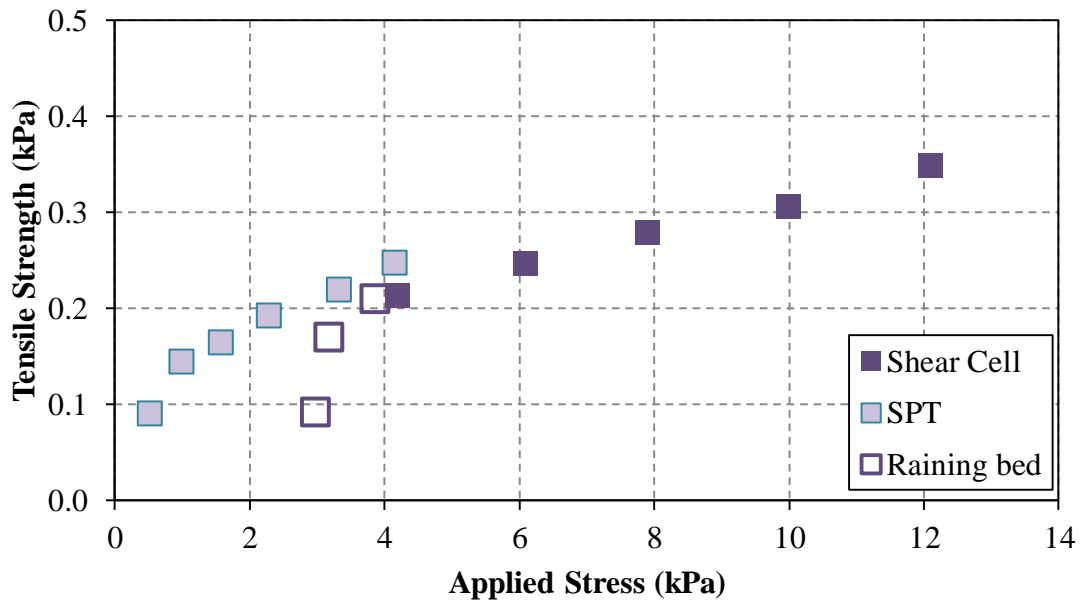


Figure 13: Comparison between shear cell, Raining Bed and SPT techniques for Respirose SV003 sample.

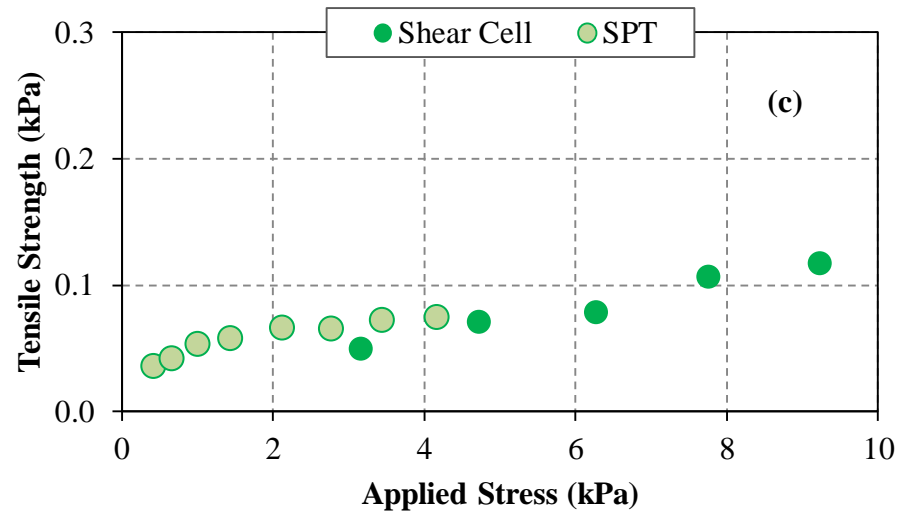
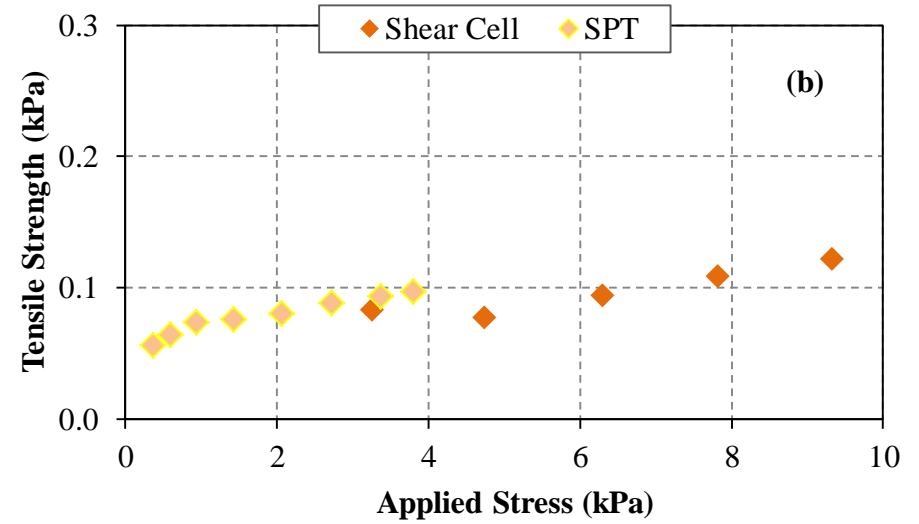
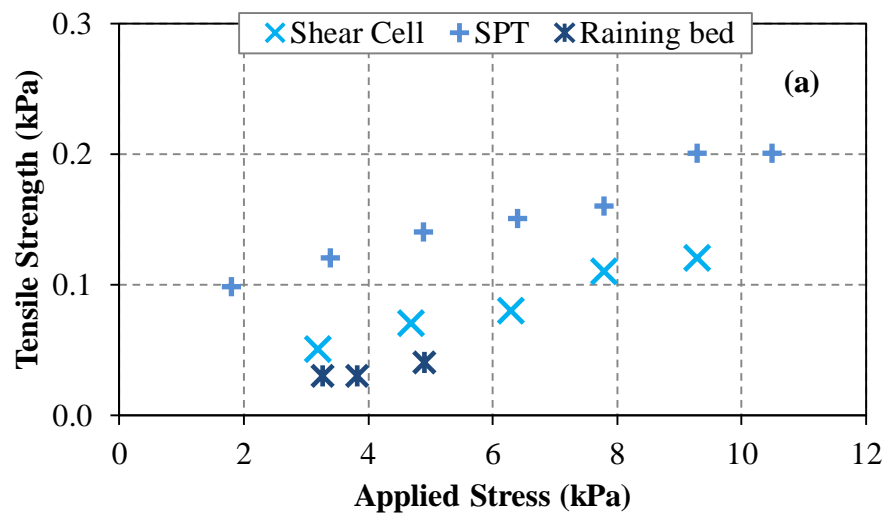


Figure 14: Comparison between techniques for (a) FCC 45-63 μm , (b) FCC 63-75 μm and (c) FCC 75-90 μm .

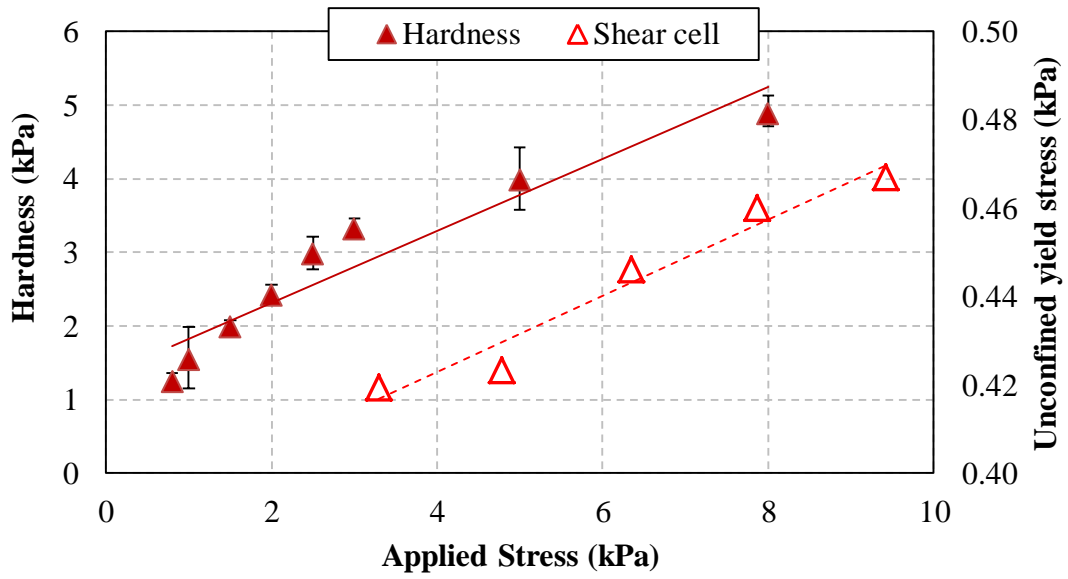


Figure 15: Comparison between shear cell and BIM for glass beads sample.

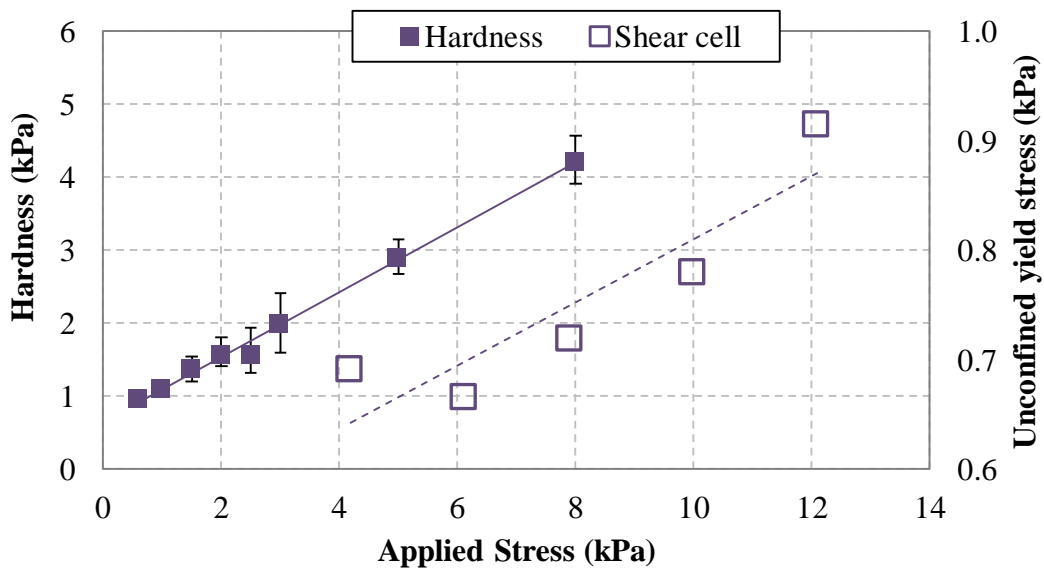


Figure 16: Comparison between shear cell and BIM methods for Respiritose SV003.

Table 1: Size distribution of test materials by laser diffraction method using Malvern Mastersizer 2000 (wet method).

Material \ size (μm)	d₁₀	d₅₀	d₉₀
Glass ballotini	11.2	44.0	94.7
Respitose SV003	28.7	62.1	98.6
FCC (45-63 μm)	38.6	55.9	74.8
FCC (63-75 μm)	53.2	69.7	85.2
FCC (75-90 μm)	64.2	87.0	107.3

Table 2: Flow function (ffc) for different materials tested.

Material	Flow function (ffc)	Evaluation
Glass ballotini	8 -20	Easy flowing – free flowing
Respitose SV003	6 – 13	Easy flowing – free flowing
FCC (45-63 μm)	31 – 70	Free flowing
FCC (63-75 μm)	45 – 66	Free flowing
FCC (75-90 μm)	33 – 77	Free flowing